2. ACCELERATOR AUGMENTATION PROGRAM

2.1 LINAC

S.Ghosh, R.Mehta, G.K.Chowdhury, A.Rai, P.Patra, B.K.Sahu, A.Pandey, D.S.Mathuria, S.S.K.Sonti, K.K.Mistry, A.Sarkar, J. Zacharias, P.N.Prakash, Pelletron Group, Cryogenic Group, D.Kanjilal and A.Roy

2.1.1 Activities related to LINAC Cryostat

To increase the energy of the ion beam from the Pelletron of Inter University Accelerator Centre (IUAC), a niobium based superconducting (SC) LINAC [1,2] is under construction. In past, pulsed silicon beam from the Pelletron had been accelerated through five resonators of the first LINAC module. However, due to various problems, the accelerating fields achieved from the resonators were less and therefore the energy gain measured from the acceleration was also found to be lower than the designed goal [3]. The major problems faced during the last on-line beam acceleration were properly diagnosed and a number of modifications were implemented to solve those problems. After a couple of successful off-line cold tests of the resonators in LINAC cryostat, ion beam from Pelletron accelerator had been further accelerated twice by the first module of LINAC and the the beam had been delivered for two different experimental groups to conduct experiments.

2.1.1.1 A few modifications to ensure the smooth operation of LINAC

Modification of power coupler

Fig. 1. Three different drive couplers were fabricated and tested to solve the problem of the old drive couplers

During the operation of the SC resonators in the first cryo-module, it was observed that due to presence of microphonics in the ambiance of cryostat, a larger frequency window (±50 Hz) was necessary leading to requirement of strong over coupling and that demanded larger forward power (150-300 watts) from the amplifier. The usage of high power for a prolong duration of time resulted to metal coating on the inside surface of the niobium power coupling port and the drive coupler. This metal coating was found to be evaporated from the "rack" of the travel mechanism of

the drive coupler. To solve this problem, three different drive couplers (as shown in figure 1, 2 and 3) were designed, fabricated and successfully tested with superconducting resonators. A number of cold tests, with the new drive couplers showed no evidence of metal coating. Functionally, all the three drive couplers are fine but more tests are still necessary to pick up the best coupler out of the three for the long term operation of the LINAC.

Control of mechanical damping of the resonator by an innovative method

Due to presence of microphonics in the ambience of LINAC cryostat, the frequency window for locking a resonator is pretty large (±50 Hz) which demands lowering of loaded Q-value of the resonator by a factor of hundred by overcoupling the drive coupler. This is done with the price of increasing the forward power from the amplifier and typically a forward power of 200-300 watts was necessary to lock a resonator in the past. To control this vibration, ordinary polished stainless steel balls of diameter 4.0 mm were inserted in the central conductor and they stayed at the end of the drift tube. Due to the presence of vibration in the cryostat, the mechanical mode of the resonator (~67 Hz) would be excited. The dominant lowest mode is the vibration of the central conductor with its anti-node at the free end, where the SS-balls rested. The dynamic friction between the balls and the niobium surface acts to dampen the oscillation, reducing the amplitude as well as the decay time of the vibration of the mechanical mode substantially. With this damping mechanism, many experiments have been conducted at room temperature and at 4.2 K and a reduction of 50% in Δf and forward power was observed repetitively in all the measurements. During last one year operation of the resonators in LINAC cryostat, most of the QWRs were locked at fields ~ 3 to 5 MV/m with ≤100 watts of forward power as shown in figure 2.

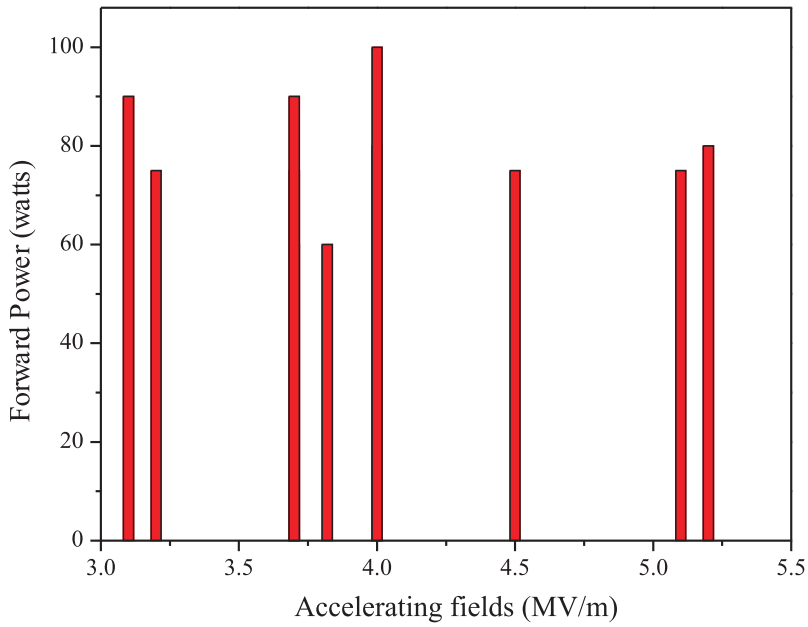

Fig. 2. Value of accelerating fields of the resonators (Phase and amplitude locked) in LINAC cryostat with the required RF forward power after implementing the damping mechanism on the resonator.

Enhancement of the cooling efficiency of the resonator

During most of the offline cold tests of the resonators in the past, a drastic reduction of the accelerating field of the SC resonators between the LINAC cryostat compared to the field obtained in test cryostat was recorded. When the resonators attained high electric field in LINAC cryostat, bubbles get formed on niobium surface immersed in LHe. These bubbles could be trapped above the top niobium flange of the resonator and under the stainless steel flange placed at ~ 15 mm above the niobium flange. That could increase the local temperature appreciably to affect electric field. To avoid this, a dome structure was installed on the top of the resonators so that if the bubbles are formed they won't be in the vicinity of the top niobium plates which carry maximum current on energizing the resonator. With this modification, the accelerating fields of the resonators measured in LINAC cryostat are in the range of 3 - 6 MV/m at 6 watts of dissipated power at critically coupled condition of the power coupler. Now the difference between the measured accelerating field of a resonator in test and LINAC cryostat has been limited to 10-20%, whereas in the past, without the cooling modification, ~50% reduction in accelerating field in LINAC cryostat has been recorded in most of the cases.

Modifications of the mechanical tuner

To improve the ruggedness of the whole system, the mechanical assembly of the frequency tuner of the resonator was substantially changed. The modification has eliminated the indium joint which used to be a source of vacuum leak and a limitation of the baking temperature of the resonator. The new design also helps to keep the resonance frequency more reproducible during many cycles of periodic warm and cool down. The new mechanical assembly of the tuner has been successfully used with the resonators in the superbuncher and rebuncher cryostats along with the LINAC QWRs.

2.1.1.2 Beam acceleration through the first LINAC module

After incorporating all the modifications, a couple of off-line tests followed by on-line beam acceleration were performed. In both the off-line tests, the performance of the resonators was satisfactory and all of them have performed at ≥ 3 MV/m at 6 watts of input power. To measure the energy and time width of the beam, two scattering chambers are placed before and after the LINAC cryostat. Surface barrier detectors were placed in both the chambers to measure the time and energy of the scattered particle from the thin gold foil. During beam acceleration, $^{28}Si^{+10}$ beam of 130 MeV from Pelletron accelerator was pre-bunched to ~ 1.5 nsec by the Harmonic buncher located in the pre-tandem region and the High Energy Sweeper located in the post tandem location. Then with a careful optimization of the phase and amplitude of the resonator acting as a superbuncher, the bunched beam was further compressed to ~ 230 psec at the entrance of LINAC cryostat.

This narrow time width beam was then injected into the first resonator operating at its highest achievable field and its phase is adjusted to optimize the energy gain. In this way, one by one, all the five working resonators out of eight of the LINAC cryostat were turned on with the optimized phase to get the maximum energy gain. A total energy of 151 MeV was obtained with an energy gain of 21 MeV from LINAC with an average accelerating field of ~ 3.1 MV/m from five

resonators [figure 3]. The ion beam of 28Si+10 beam of 130 MeV from the Pelletron accelerator had been accelerated twice, in September and November 2006. During both the time of beam acceleration, Si beam of ~ 150 MeV was supplied to two experimental groups to perform experiments in two different beam lines. Right now, more cold tests are being carried out on the resonators in LINAC cryostat to verify the reliability of the whole system. We are hopeful that within a few months all the eight resonators can take part in the beam acceleration and the average energy gain from the first cryomodule is expected to be 4 MeV per charge state.

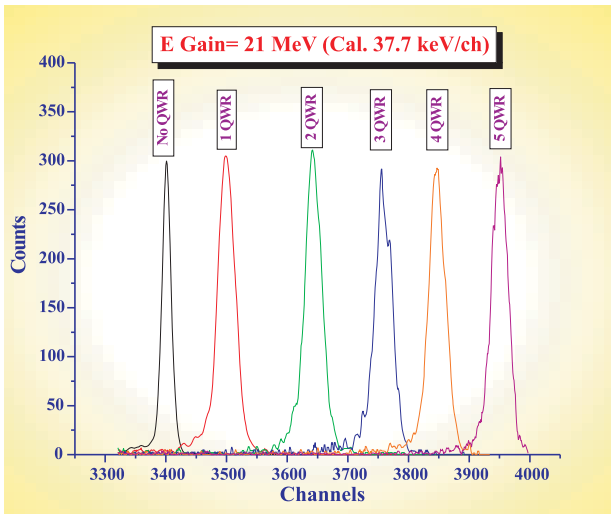

Fig. 3. The energy of 28Si beam measured before LINAC and after LINAC, with the resonators turned on one by one during the beam acceleration in September and November 2006

2.1.2 Activities related to Rebuncher cryostat

Fig. 4. Figure shows two QWRs loaded in the rebuncher cryostat prior to their first offline cold test

The activities related to the rebuncher cryostat, has also been carried out during 2006. Two resonators, one of which was fabricated in-house, were installed with all the modifications mentioned above and tested for the first time in rebuncher cryostat at liquid helium temperature. Accelerating fields of 3.3 and 3.7 MV/m were measured for the resonators at 6 watts of input power for the resonators made indigenously and made in collaboration with Argonne National laboratory, respectively. The frequency tuning ranges of the resonators were measured to be 120 and 80 KHz and the mid frequencies of both of them were centered nicely around 97.000 MHz. It is expected that within a few months, during the beam acceleration by the resonators in LINAC cryostat, both the resonators in rebuncher cryostat will be used to deliver a properly bunched beam to the user.

REFERENCES

[1] P.N.Prakash et al, Pramana - journal of Physics, Vol. 59, No. 5, Nov. 2002. page 849-858.

[2] S.Ghosh, R.Mehta, P.N.Prakash, A.Mandal, G.K.Chaudhari, S.S.K.Sonti, D.S. Mathuria, K.K.Mistry, A.Rai, S.Rao, P.Barua, A.Pandey, B.K.Sahu, A.Sarkar, G.Joshi, S.K.Datta, R.K.Bhowmik and A.Roy published in Pramana, J. of Physics, Vol. 59, No.5, Nov 2002, page - 881.

[3] S.Ghosh, R.Mehta, G.K.Chowdhury, A.Rai, B.K.Sahu, A.Pandey, D.S.Mathuria, S.S.K.Sonti, K.K.Mistry, P.Patra, S.Ojha, A.Sarkar, R.Joshi, P.N.Prakash, A.Mandal, D.Kanjilal and A.Roy, Proc. of Indian Particle Accelerator Conference 01-05 March, 2005, Kolkata, India, page 48.

2.1.3 Superconducting Niobium Resonators

P.N.Prakash, S.S.K.Sonti, K.K.Mistri, J.Zacharias, D.Kanjilal & A.Roy

The production of fifteen quarter wave resonators for the second and third LINAC modules has progressed as per our plan. In addition to the resonator production, two ANL built resonators and one indigenously built resonator are being repaired.

2.1.3.1 Resonator Production for the 2nd & 3rd LINAC Modules

The production of fifteen quarter wave resonators for the 2nd and 3rd LINAC modules

Fig. 1(a) Niobium Outer Housings

Fig. 1(b) Drift Tubes (top) & Loading Arms (bottom)

has advanced satisfactorily. Figure 1(a) shows the niobium outer housings and figure 1(b) shows the drift tube and loading arm cylinders (the capacitive and inductive parts of the central conductor assembly respectively). The niobium top flange, which joins the central conductor to the outer housing, for all the resonators have been machined and the outer stainless steel vessels are nearing completion. The niobium-stainless steel flanges for the open-end of the resonators will be ready shortly. Fabrication of the niobium slow tuner bellows has just begun. The assemblies in fig. 1b are now getting electropolished. The electropolishing (EP) is being done in sets of three to reduce time and effort. The electron beam welding work is also carried out with multiple welds in a single pump down to save time and effort. In all about 250 welds have been performed using the in-house e-beam welding facility. This represents approximately 70% of the e-beam welding work for completing the basic niobium resonator, and about 58% of the entire fabrication work that includes the slow tuner bellows. We plan to complete the fabrication by the middle of this year (2007).

2.1.3.2 Major Repairs on QWRs

Last year we had planned to modify the drift tube of one of the indigenously built quarter wave resonators (of the two) to convert it into a b=0.09, 109 MHz resonator for multipactoring studies. However, during the electropolishing of the other indigenously built resonator the niobium surface got severely etched because of incorrect labeling of the electropolishing solution. Prior to the accident this resonator had performed above the nominal design goal in cold tests. However, after the accident its performance deteriorated substantially and as such it is not usable in the LINAC. We are trying to see how this resonator can be salvaged. In the mean time the idea to convert the first resonator for multipactoring studies was dropped and we have now reverted back to the original design. This decision has been taken to ensure that sufficient number of resonators are available for the superconducting LINAC. The drift tube on this resonator, along with two others, are currently being repaired. For this the resonators have been cut open from the shorted end to access the central conductor assembly. This is a major work and it has been clubbed with the on-going resonator production since there is some similarity between the resonator fabrication and the repair work.

2.2 CRYOGENICS

T.S.Datta, J.Chacko, A .Choudhury, J. Antony, M. Kumar, S. Babu, S.Kar, R.S.Meena, and A.Roy

In this academic year, four cold tests have been performed for resonators in the beam line cryostats of RF-Superconducting LINAC. Beam was accelerated through the 1st LINAC module twice in this year. First time close loop cooling of all the three beam line cryostats together have been performed successfully by helium distribution network. A series of experiments have been carried out in Multilayer Insulation (MLI) calorimeter and the heat load between 80K and 4.2K has been reduced from 60mW to 16mW. Similarly experimental data have been generated with thermosyphon cooling by liquid nitrogen and analyzed with respect to level , flow rate and heat load. A low cost coil winding facility with flip mechanism has been designed and developed for superconducting quadrupole magnet of HYRA project. Liquid nitrogen plant upgradation work

has been initiated in this period. Technology of some cryogenic instruments developed in house has been transferred to private firms for bulk production and supply. Proposals on development of cryo-free magnet and recovery of helium gas from monazite sand have been submitted to DST and BRNS respectively.

2.2.1 Cryogenic Facility

I. Liquid Helium Plant

The helium plant was operated five times out of which four runs were in close loop mode for off-line testing of the resonators and beam acceleration through LINAC. Average duration of each run in close loop mode is approximately twelve days. Estimated total production of LHe was ~ 100000L and the running hour is 1100hr. which is higher in comparison to last year as shown in fig.[1]. A new speed controller has been developed to substitute the Fincor speed controller for the cold expander. Performance is satisfactory and there is a plan to have a similar one for warm engine.

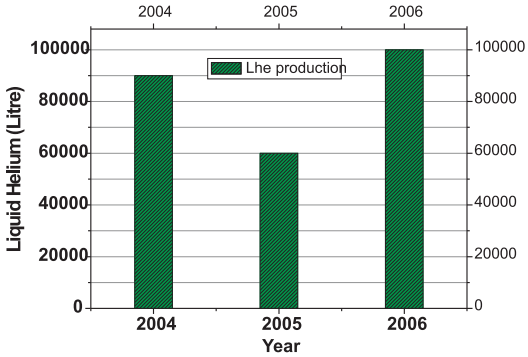

Fig. 1. Bar Chart of LHe Production

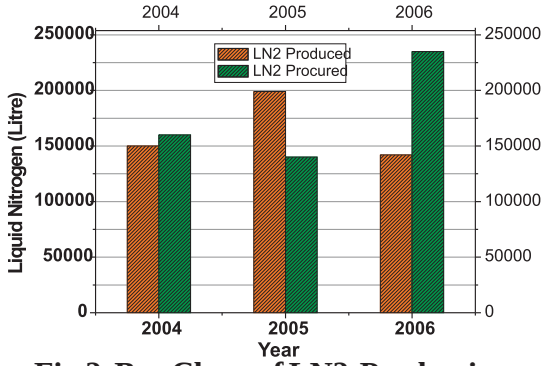

Fig.2. Bar Chart of LN2 Production

II. Liquid Nitrogen Plant

To meet the enhanced demand of liquid nitrogen on account of prolonged off-line and beam acceleration test in LINAC, upgradation of liquid nitrogen plant was planned in the previous year. Modification is achieved by using stand-by four cylinder cryogenerator along with upgradation of PSA capacity from 40M3/hr to 100M3/hr. The new PSA is of modular type, compact and filled with dual type regenerative drier in place of refrigerated air drier. Preliminary installation and integration of new system with existing one has been completed. Fig.[3] shows some of the newly installed systems of upgraded LN2 plant. Final commissioning and performance test will be carried out shortly.

In this year the in-house liquid nitrogen production was 1,42,000 L which is significantly lower than last year which is shown in the fig.[2]. LN2 procured from outside vendor was ~2,35,000 L. The Plant was shut down for four months on account of up-gradation work.

A forty-meter long flexible LN2 filling line was connected to the external LN2 storage tank for temporary filling of LN2 from the tanker standing outside the boundary wall of the campus as the approach road to the external LN2 storage tank was blocked because of construction work.

Fig.3. New PSA system of upgraded LN2 Plant

III. Helium Gas Purifier and Recovery System

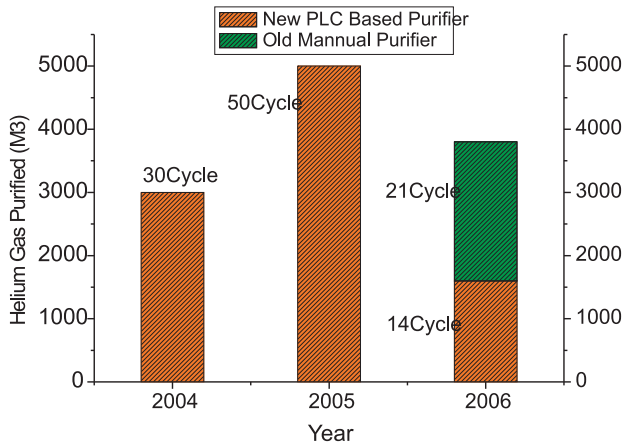

Fig. 4. Bar Chart of Helium Gas Purification

The old manual purifier was made operational when a leak was developed in the charcoal bed of the new PLC based automated helium gas purifier after 12500M3 of helium gas purification for last four years. The old purifier was integrated with helium gas recycling system incorporating few additional features like on-line drier, temperature sensors to monitor LN2 level

and manifold system to analyze purity of helium gas. With this arrangement, it was possible to purify 2200M3 impure helium gas in 21cycles as shown in the fig.[4]

The leak, developed in the PLC based automated purifier, has been rectified and it is currently undergoing through the actual cold tests. It will be in operation once it passes through the cold tests.

2.2.2 Performance Report of Cryostats

LINAC Cryostat

Four cold tests have been performed with 8-QWRs in the 1st LINAC cryostat. The beam was accelerated through this LINAC module twice in this year.

Heat Load Analysis of 1st LINAC Module

The measured static heat load of 1st LINAC Module at 4.2K is higher than the expected which was reported earlier. Detailed experimental measurements were carried out to analyze the unexpected parasitic heat load to the liquid helium system. Rf- Drive couplers and the aluminum support structure of resonators were found to be the major contributors to the parasitic heat load at 4.2K.

The heat flow through each drive-coupler is calculated by measuring the temperature profile along the drive-coupler for both static (i.e. no RF power) and dynamic condition (i.e.70W-200W RF power). The calculated load comes about 0.5W and 1.4W per drive-coupler with and without RF power.

In the present LINAC cooling methodology, Aluminum support bars (total weight~160Kg) are precooled up to 150K by liquid nitrogen and no further precooling is followed by forced flow of cold helium gas through the precooling channel. Hence a wide temperature gradient exists between aluminum bar and resonators at 4.2K. This is because of higher contact resistance and large mass with higher specific heat of aluminum bar. On careful analysis of temperature profile of aluminum bar, it is observed that the temperature drops ~8K/day for first 5-6days and then 4K-5K/day. The heat load, calculated from the temperature drop, is 10-12 W with eight resonators and one solenoid magnet. It is also confirmed that the load is almost proportional to the number of resonators.

Rebuncher Cryostat

The off-line testing of the Rebuncher cryostat with two resonators was performed in this year. The lower annular LN2 vessel has been replaced by the copper thermal shield to accommodate the extra length of new drive-coupler. The shield is cooled by gravity flow and the cooling manifold has been modified to suit the existing line. The performance is satisfactory. Figure [5] shows the typical variation of copper shield temperature with LN2 level in the upper vessel. It is also noticed that the required helium cooling time is much higher if bypass cooling mode is not followed.

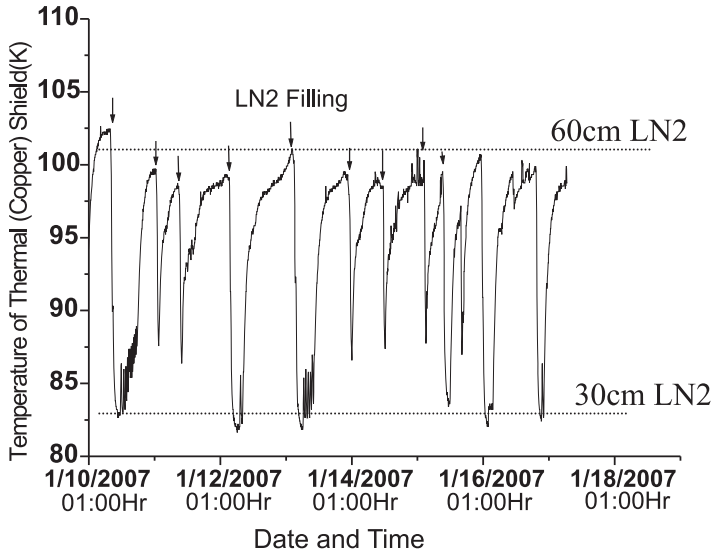

Fig. 5. Temperature profile of the copper thermal shield of Rebuncher cryostat

2.2.3 Other Experimental Studies

I. MLI experimental setup

A series of experiments have been performed to measure heat load between 78K to 4.2K and various layers of MLI, Al tape and on bare surface. The effort, made to reduce the heat load on the experimental vessel from 78K- 4.2 K, was reasonably successful. Finally the static heat flow got reduced to 16mW from its initial value 60mW. Some precautionary modification as described below on experimental set-up is reason behind it.

a. A circular copper flap (0.5mm thick) around the top liquid nitrogen guard vessel which ensures blocking of direct radiation to experimental vessel from top plate through the annular gap of the cryostat.

b. Thermal anchoring of the top of the experimental vessel from the pipe connecting two guard vessels to experimental by two numbers of 1" copper braid.

c. Removal of both diode sensors from the experimental vessel and this contributes about 6mW.

The achieved 16 mW of load at 4.2K (so far best result) is a combination of radiation and conduction load (assuming that gas conduction is negligible at vacuum level of 10^{-6} torr). A novel technique was followed to separate out the above two contributions. Different temperature (~64K) was achieved at the annular shield by pumping down the annular LN2 vessel, therefore the radiation load was varied (assuming that emissivity of metal does not change very much from 78K-64K) but conduction load was kept constant as shown in fig.[6]. From these two experimental observations , it is concluded that the radiation, between 80K and 4.2K with aluminum tape on SS, contributes 6mW (30mW/M2).

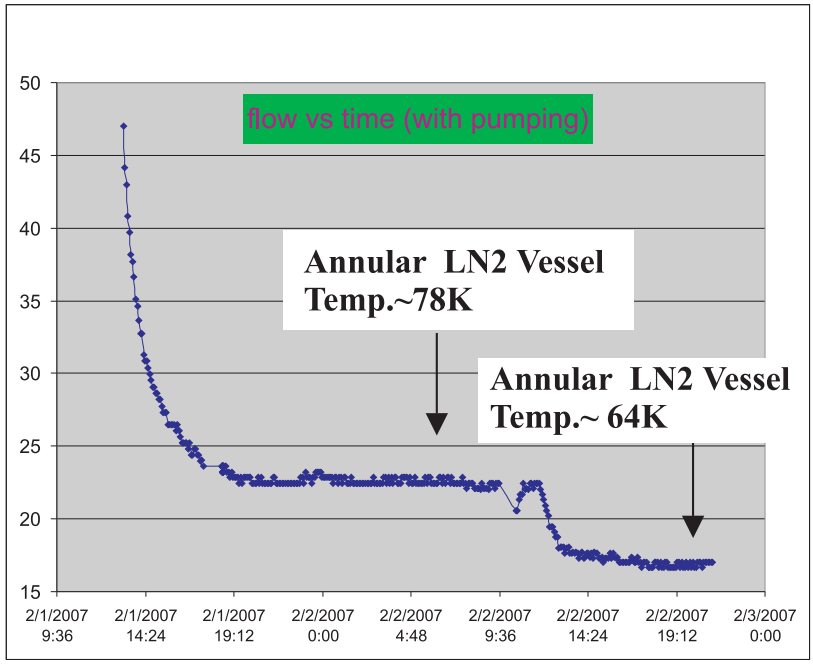

Fig. 6. The effect on annular LN_2 vessel temperature on the LHe evaporation rate

Another experimental observation shows head load of ~25 mW at 78K-78K (LN_2-LN_2) configuration which should be ideally zero. This might be due to the conduction through the filling tube wall. A periodic oscillation of flow rate (cc/min) has been observed (peaking at around 3 AM/PM) as shown in fig.[7]. The reason behind this is not yet clearly understood.

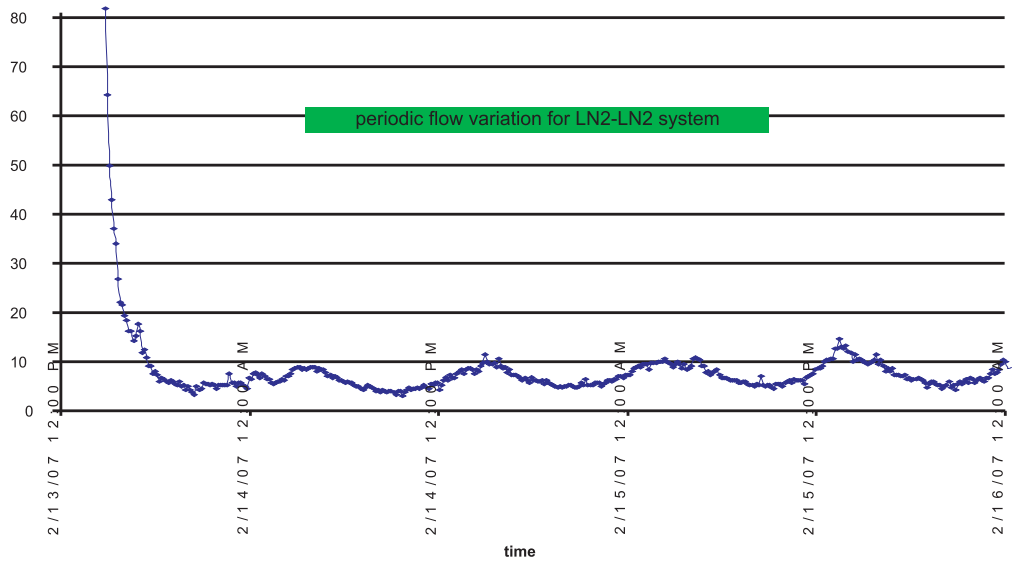

Fig. 7. Periodic flow variation for LN_2-LN_2 System

II. Gravity Cooling Experimental set up

This experimental program has been initiated to evaluate and generate input design parameters for the optimized performances of cryostat thermal shield cooled by gravity flow. In the experimental set up, the stabilized temperature of shield at different heat load has been found for existing copper clamping mechanism. The stabilized temperature increases linearly with the heat load of the shield as shown in fig.[8]. The rise in temperature with liquid level reduces as the heat load increases because of increased liquid flow through the shield for higher load. Fig.[9] shows the variation of temperature with the liquid level for different heat load. The analytical relation between liquid level, heat transfer coefficient and contact resistance of the copper clamp is being developed.

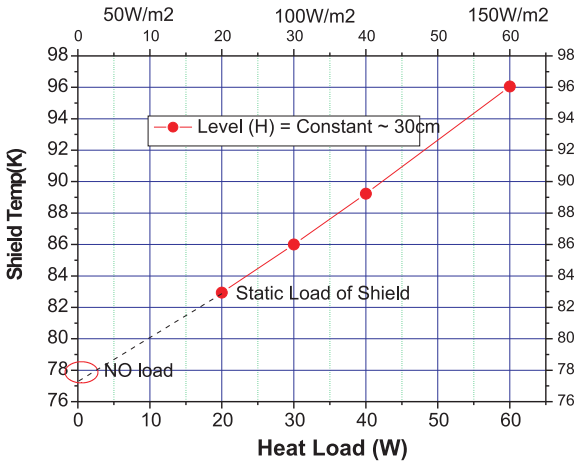

Fig. 8. Stabilized temperature of thermal shield for different heat load (full liquid level)

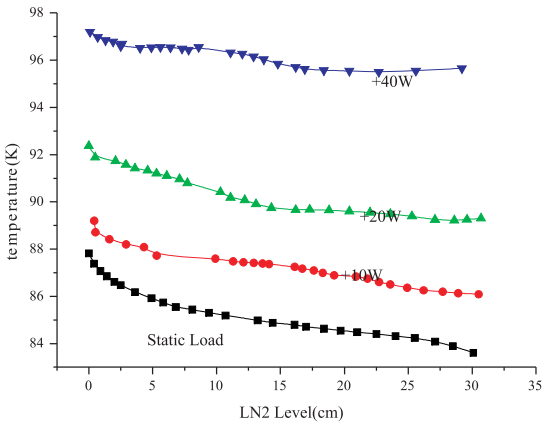

Fig. 9. The rise in temperature with the liquid level for different heat load

2.2.4 Other Developments

I. LN_2 Driven Car

The successful development of prime mover by using liquid nitrogen as a fuel has been reported earlier. Same program was extended to demonstrate running of a vehicle by using clean liquid nitrogen fuel in collaboration with DCE, New Delhi. A single cylinder100cc air cooled four stroke petrol engine of Hero-Honda motorcycle has been modified into two stroke expansion cycle. The LN_2 tank (capacity ~14litres) is pressurized by passing the LN_2 through the heat exchanger where it absorbs the heat from atmosphere and finally it injects the high pressure gas into the expansion engine through a flow meter. The indigenously developed car with a novel concept rolled down to few hundred meters in IUAC campus as well as DCE campus. The performance efficiency and the fuel economy is yet to be established.

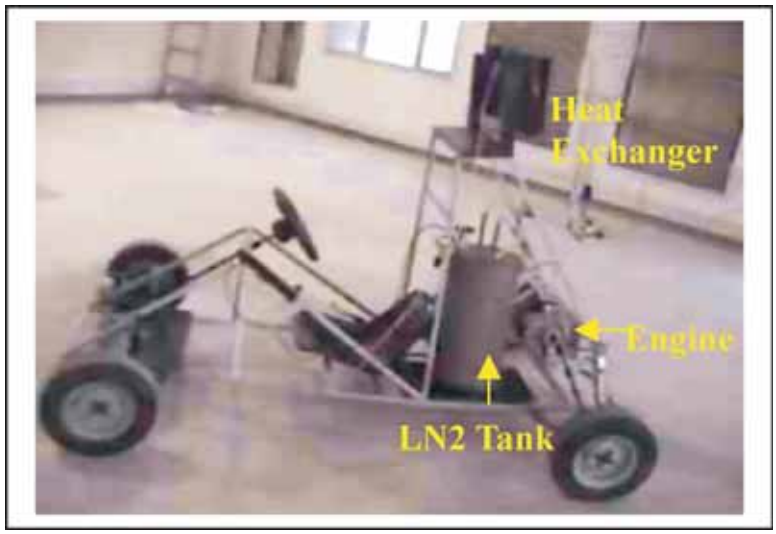

Fig. 10. Picture of LN2 driven demo-car

II. Development of Superconducting Quadrupole Magnet

A wide bore (200mm) cold iron superconducting quadrupole doublet magnet with cryostat is being developed at IUAC for the HYRA project funded by DST. A coil winding machine with a flipping mechanism has been designed and developed to make the Nb-Ti superconducting coils. As a first step a sample coil has been made using 1mm. diameter. copper wire. Using a special mechanism the stycast epoxy coating is done while the winding is in progress. Necessary winding formers and fixtures are locally developed to get the desired shape and size of the coil. Few more sample coils will be made using copper wire with epoxy before the actual winding with superconducting wire. The final design of the cryostat will be taken up shortly after the coils are mounted. A comprehensive report on present status of HYRA is presented in Section 4.3.2 .

Fig. 10A. Flipping mechanism of winding machine

Fig. 10B. Winding Formers

2.2.5 FPGA based Cryogenic Instrumentation and other Electronics Development

Joby Antony and D.S. Mathuria

Different cryogenic instruments have been developed in-house using FPGAs for various cryogenics applications at IUAC. Technology of some of these instruments have been transferred to a private firm (M/s NVIS technologies, Indore) for mass production and a few of them are being used by NPL, New Delhi for their low temperature measurements.

Fig. 11. Cryogenic instruments developed at IUAC

I. Multi channel Cryogenic Temperature Monitor

Cryogenic temperature monitors of sixteen and eight channels have been designed and developed for Silicon diodes and Platinum sensors in the temperature range of 3.2K-410K and 77K-410K respectively. PC Interfaces like RS232 (Optically isolated), USB and Ethernet converter O/P are also provided. Big LCDs have been used for simultaneous temperature readouts.

II. LINEARIZER UNIT with 16 linear Analog Outputs

This is a linearizer unit which can produce 16 linear 0-10V outputs proportional to different non-linear inputs. It has got an analog front-end for low signal conditioning, input multiplexer unit and 16 DACs for simultaneous linear outputs. RS232 interface is also provided in this instrument.

III. Current sources for Cryogenic applications

Two precise current sources have been developed for cryogenic related calibration jobs. This includes programmable 0-100mA and 4-20mA generators.

IV. Mass flow readout meter & flow-viewer software for nitrogen and helium gas.

It is an instrument developed to display and log the flow of N2/He gas using SENSIRION ASF1430 sensor used for MLI experimental set up. The flow is measured from a 16-bit binary number using SPI bus interfacing using FPGA and displays it on a 16*1 LCD display. A Flow-

Viewer Software is also developed using Labview to replace the software supplied by the company which was not suited for low frequency data logging using RS232 interface. Different calibration curves for nitrogen and helium can be selected from the front panel of the instrument.

V. A prototype CAMAC controlled drive probes

This is a prototype setup made to study the feasibility of controlling the resonator drive probe through CAMAC interface. It had an existing single channel controller to run a single Drive probe at a time manually and now it has been modified to run through a PC using CAMAC. But it had some limitations which will be overcome in a new type of drive probe controller which is built for simultaneous movement of all 8 drive probes manually as well as remotely. The GUI below shows the control panel.

Fig. 12. GUI for RF Drive coupler control for resonator

VI. Gamma Radition Display Meter

Joby Antony, Birendra Singh

This is a digital display unit installed to replace the existing 16 analog gamma radiation monitors in Pelletron control room. Now it has 16 independent 16*1 character displays to display the gamma radiation at different levels in pelletron with a display resolution of 0.01 mR/hr. It has 16 low level 0-100uA nonlinear inputs. RS 232, Ethernet interfacing O/Ps have been provided for local monitoring.

Fig. 13. Digital gamma radiation display at Pelletron control room

VII. An End -window GM counter for data logging

This is a project required by HP group for Environmental Sample Analysis. This is an End-window GM counter to count the number of TTL pulses generated out of a GM detector in counts/sec or counts/min. This device generates the real time clock in seconds/minutes, counts/sec & counts/min and the corresponding continuous data is displayed on a 16*1 character display and transmits these information serially to PC.

2.3 RF ELECTRONICS

A. Sarkar, S. Venkataramanan, B.K. Sahu, K. Singh, A. Pandey, Y. Mathur, P. Singh and B.P. Ajith kumar

2.3.1 Status Report of the Multi-harmonic Buncher & the High Energy Sweeper and associated jobs

The multi-harmonic buncher (MHB) was operated along with the high energy sweeper (HES) for the first time to provide 12 MHz pulsed beam to a LINAC User (National Array of Neutron Detectors). Earlier this system (MHB+HES) was used to provide beams only for testing LINAC. ^{28}Si beam pulses with FWHM ~1.4ns was provided to the user. The sweeper slit window was optimised and kept at 2mm. The sweeper phase had to be tuned occasionally. The entire system ran smoothly for several shifts. This system was also operated to provide LINAC beam to the HYRA beamline for a few shifts.

The multi-harmonic buncher (MHB) was also operated along with the low energy chopper (LEC) to provide 4 MHz pulsed beams to GPSC and HIRA beamlines. ^{19}F and ^{16}O beam pulses with FWHM ~ 1.2ns and 1ns respectively were delivered. Travelling Wave Deflector (TWD) was also used in the HIRA run to provide pulsed beam at lower repetition rate.

There was a vacuum problem near the MHB chamber with the pressure rising to 10^{-6} torr resulting in the closure of the beamline valve below the chamber. After a thorough investigation it was found that a soft solder joint in the feedthrough connecting the lower grid of the MHB was leaking (at 10^{-7} torr range). By spraying vacuum sealant on the joint, the leak was closed and 10^{-9} torr was easily achieved in the MHB chamber.

A water leak in the de-ionised water cooling system for the MHB was observed during a pulsed beam run. The leak was fixed. The coupler positions of the tank circuits for the MHB got disturbed during the water leak fixing. The couplers were adjusted for critically coupled positions once again and the tank circuits were retuned.

2.3.2 Operational Experience with resonator control Scheme

The resonator control scheme is used with the present pelletron control system to accelerate the heavy ion beam from tandem through LINAC. The beam is finally delivered at User end for experiment. The phase and amplitude lock of resonators are found to be stable and within specified range during the experiment. The RF calibration of resonator is done by using a commercial RF level meter from Rohde and Schwartz. The calibration matches well with the actual energy

gain by the beam. Slow -tuner control mechanism is found to be working properly to handle the slow drifts due to Helium pressure fluctuations.

The RF electronics setup for re-buncher cryostat is done this year. An off-line test using the set up is done with the re-buncher cryostat. This set up will be used in the next beam test for delivering the pulsed beam from LINAC.

2.3.3 400Watts VHF Power amplifier for LINAC

Assembly of 20 numbers of 400 watts VHF RF power amplifiers required for additional LINAC modules has been successfully completed. Various RF power blocks, control cards, cable assemblies, critical sub-assemblies like transmission line transformers, splitters and combiners were duplicated. These amplifiers are individually characterized and subjected to continuous burn-in test under extreme load and environmental conditions.

Fig. 1. 400Watts VHF Power amplifier

2.4 BEAM TRANSPORT SYSTEM

A.Mandal, Rajesh Kumar, S.K.Suman, Sarvesh Kumar and Mukesh Kumar

Beam Transport System laboratory takes care of regular maintenance, design and development of Accelerator beam Transport System. Several magnets and power supplies for them have been indigenously developed. Besides, BTS laboratory has been involved in instrumentation development for other projects particularly power supplies.

2.4.1 Beam optics for LEIBF Facility in New Low Energy Ion Beam (LEIB) Laboratory

The beam optics for LEIBF facility has been done for three beam lines 75^0, 90^0, 105^0 using TRANSPORT code up to first order and based upon that Layout of Beam hall in New LEIB building is being drawn. Here we have shown optimization for 90^0 beam line.

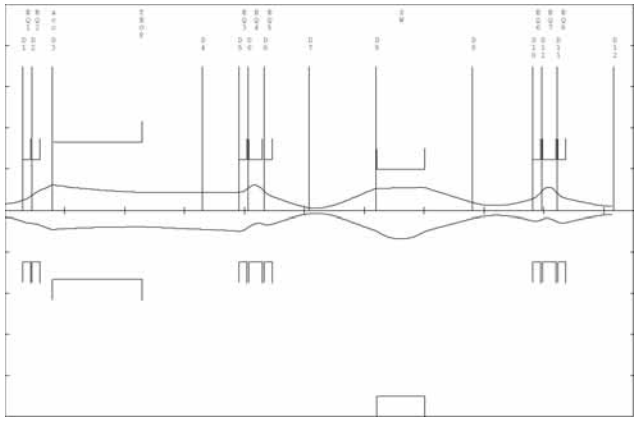

Fig.1. Beam Optics for 90^0 beamline using TRANSPORT

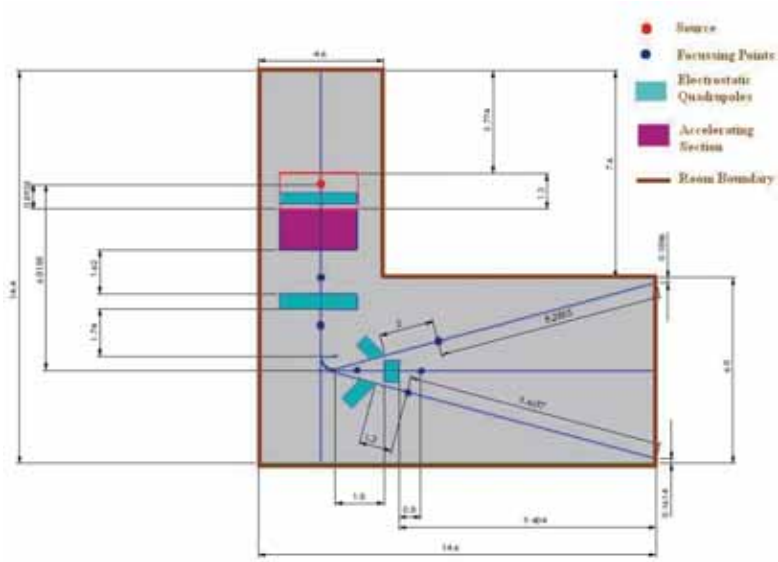

Fig.2. Layout of LEIBF Facility in New LEIB Building

2.4.2 Design of Switching Magnet for LEIBF Facility

A Switching Magnet has been designed for the LEIBF facility to switch the beam in three beam lines 75^0, 90^0, 105^0. The ion optics calculation has been carried out using simulation program GIOS & TRANSPORT CODE. A typical ion optics for 90^0 beamline is shown below. The ion optical specification of the magnet is given in table below.

Specifications for Switching Magnet

Maximum field	1.5 T
Magnet type	H -shaped
Bending Angles	75^0, 90^0, 105^0 (All bent left w.r.t beam)
Bending radius (mm)	600 (75^0), 516 (90^0), 460 (105^0)
Entrance Angle	29^0,
Exit Angles	29^0(90^0), 17^0(75^0), 46^0(105^0)
Pole gap	65 mm
Pole width	300 mm entrance
Homogeneity	Better than 10^{-3} over 30mm
Coil type	Hollow conductor (OFHC copper)
Cooling type	water
Power Supply existing (Order Placed to Danfysik)	50V, 250A

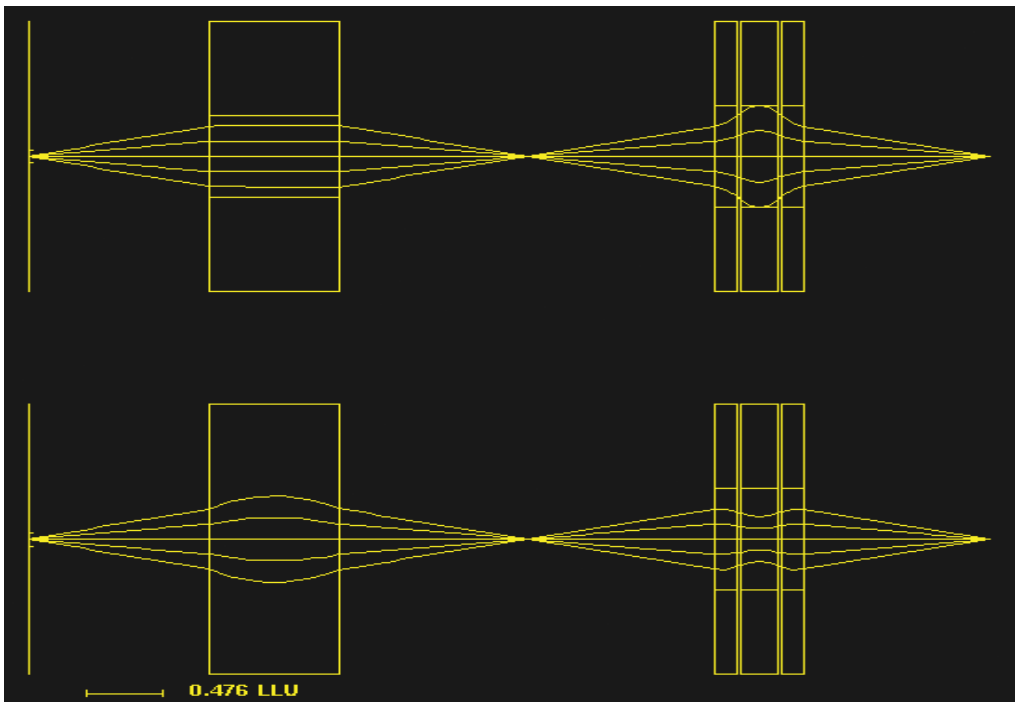

Fig. 3. Beam Optics for 90^0 beamline using GIOS

2.4.3 Fabrication and Testing of Steerer Magnets

Four steerer magnets have been have been fabricated and tested using Group 3 Hall probes for their excitation curve.

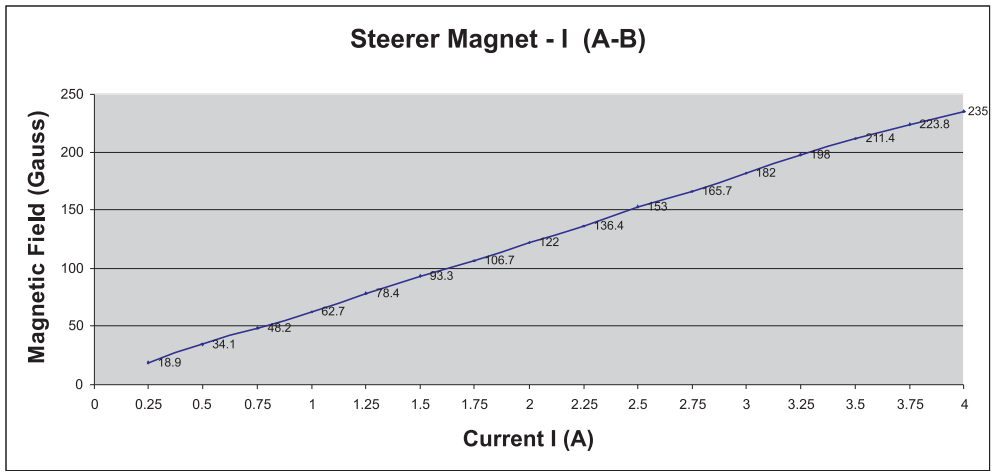

Fig. 4. A typical Excitation Curve of Steerer Magnet

2.4.4 Testing of a Large Area Scanner Magnet

The Large area scanner magnet fabricated last year has been tested for DC current using Group 3 Hall probes for its magnetic field profile and excitation curve. The magnet has also been tested with 50A, 50Hz triangular wave output from the indigenously developed scanner power supply. Temperature rise of the magnets was noted approximately 10 degrees centigrade after 10 hours.

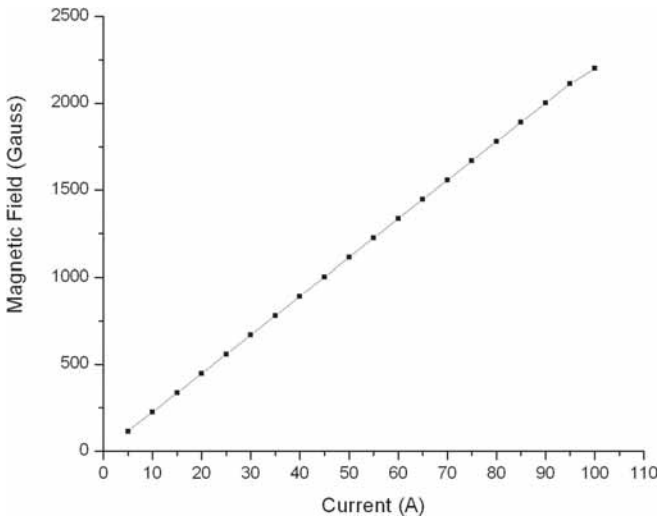

Fig. 5. Excitation Curve of Scanner Magnet

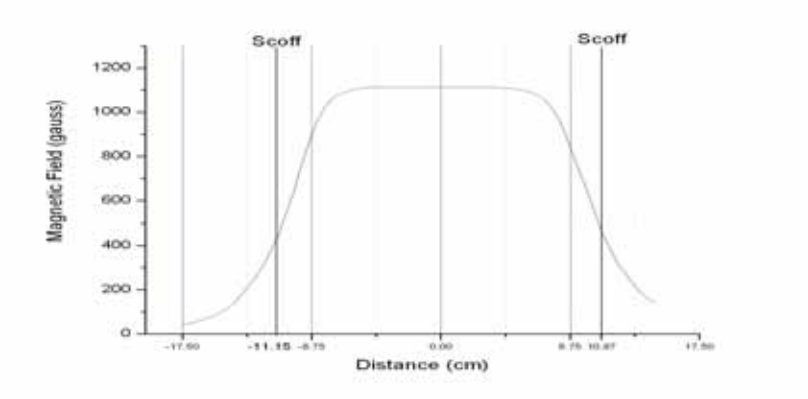

Fig. 6. Magnetic Field Profile of Scanner Magnet in Axial Direction

2.4.5 High Current Scanner Magnet Power Supply for Y-axis

Scanning magnet requires bipolar triangular wave current regulated output power supplies. These are limited bandwidth amplifier without zero cross-over distortion. Stability of regulation loop of these current regulated output amplifiers is very critical because this has to feed inductive load. Last year we had developed and tested one amplifier for x-axis (+/-50A, +/-50V, 50Hz). This year the amplifier for Y-axis (+/-70A, +/-15V, 0.4Hz) has been developed. Loop stability and oscillation problem has been solved successfully. The unit is under test with actual load for stability, thermal management and failure rates. After all these testing, soon the unit will be installed in LINAC Mat. Sc. beamline.

Specifications and features:

1. Triangular wave current output : +/- 70A
2. Output voltage range : +/- 15V
3. Scanning frequency range: 0 to 0.4Hz (4mH inductive load)
4. Triangular wave current regulated output without cross over distortion
5. Programmable foldback limits for over voltage and over current
6. Remote control through CAMAC

Fig. 7. High Current Scanner Magnet Power Supply

2.4.6 BGO Detector Bias Supply

This power supply has been developed for INGA project. This is a high voltage power supply housed in a standard double width NIM module that provides either polarity of output voltage from 0-3 kV/10 mA. It provides extremely stable low noise high voltage that is required for proper bias of photo multiplier tubes. Two feedback loops are used, one for pre-regulation which is necessary to limit the power dissipation and second loop is to regulate the output voltage. 50 nos. of such power supplies will be required and fabrication of all these units will be done in house. Design and assembly details and materials procurement has been done.

Specifications:

1. Output Voltage : 0 - 3kV
2. Load Capacity : 0 - 10mA
3. Regulation : 0.005%
4. Output Ripple : < 10mVpp

Features:

- Bipolar -selectable
- Two simultaneously available output - SHV
- Front panel LCD meter- simultaneous V-I display
- Overload and short circuit protection

Fig. 8. BGO Detector Bias Supply

2.4.7 Pre-amplifier Power Supply

This power supply has been developed for INGA project. The pre-amplifier power supply is a portable power supply ideally suited for providing power to pre-amplifiers in remote locations. The power supply provides four highly stable and low noise output voltages to six pre-amplifiers simultaneously through standard 9-pin connector on the rear panel. 15 nos. of such power supplies will be fabricated in house. Assembly details, drawing and material procurement has been completed.

Specifications:

- Outputs : +12V/ 1A, +24V/1A, -12V/ 1A, -24V/1A
- Regulation : < ±0.05 %

- Noise & ripple : < 3mVpp

Features:

- Foldback Output current limit
- Thermal protection

Fig. 9 : Pre-amplifier Power Supply

2.4.8 Power Supplies for HYRA Quadrupoles

Design and prototyping for four numbers of high current high stability (300A, 45V) power supplies has been finalized and tested successfully. These magnet power supplies are DC current regulated supplies designed for applications requiring very high stability. The power supply control electronics has been designed in modules for ease of maintenance. Materials have been procured and all assembly drawings have been finalized to fabricate 4 nos. of such power supplies.

Specifications:

- Power range : 10kW- 12kW
- Current range : 300A
- Voltage range : 32V and 42V
- Long term stability (8hrs) : 20 PPM

2.4.9 Controller for Spark Counter and Beta Ray Spectrometer

Spark Counter and Beta Ray Spectrometer have been indigenously developed for M.Sc. teaching lab. The controller has been developed keeping in view that it can control both Spark Counter as well as Beta Ray Spectrometer. It provides 0-5 kV bias voltage to the detector of Spark Counter and 0-500 V to Beta Ray Spectrometer's detector. The controller contains pulse detecting circuit, pulse shaping, decimal pulse counter and timer. Pulses corresponding to the detected particles are generated in the controller which are counted and displayed for the set time period. The controller has following specifications and features.

1. Output : 0-5kV, 100μA for spark counter (SHV connector).

   0-500V, 100μA for Beta-ray spectrometer (BNC connector).

2. 4 digit pulse counter for max. count ~9999
3. 3 digit presettable timer for time setting from 999-000 second.
4. Panel meter for bias voltage display.

Fig. 10. Controller for Spark Counter and Beta Ray Spectrometer

2.4.10 STM Unit Power Supply

This unit has been developed to power indigenously developed STM. It provides highly stable and low noise DC outputs. Fixed Voltage regulator circuits are used to regulate the output voltage. Special grounding technique and sense terminals are used to achieve low noise and high stability. Output adjusting facility is provided to adjust the output within ±10% of the rated value.

Specifications:

- DC Outputs :±15V /1A, ±15V/200mA, +5V/1A, +5V/1A, ±200V/40mA

Fig. 11. STM Unit Power Supply

2.4.11 INGA and HYRA power supply Fabrication

BTS lab has developed high voltage detector bias power supplies for INGA and high current power supplies for HYRA. Prototype of all these developed power supplies have been tested and found satisfactory. All these units are required in large quantities; hence it is decided to assemble all the required quantity in house. For that complete assembly details, drawings and scope of works has been documented to setup the production line. Materials and components have been sourced and procured. Assembly process will start very soon.

Details of units to be assembled:

- 3kV, 10mA HV supply for BGO detector - 40 nos.
- 5kV, 100µA HV supply for Ge Detector - 50 nos.
- Pre-amplifier power supply - 15 nos.

- 300A, 45V HYRA Quad PS- 4 nos

2.4.12 Instrument development in progress

- **Universal Regulation Module for Magnet Power Supply:**

Beam transport system requires different types of power supplies which are low current, high current, unipolar, bipolar etc. Hence many types of spares and electronic cards have to be kept in stock. To keep the inventory of spares low, we are designing a universal regulation module and electronics which can control all types of power requirements so that we can have adequate control of all spares availability and maintenance. Design has been completed and implementation is in progress.

- **Electric Field vs Polarization measurement system:**

Development of EP system for characterization of ferroelectric materials for Mat. Sc lab is in progress. The system will consists of following specifications and features.

- Electric field upto 0-1kV / cm
- Triangular wave excitation
- Frequency range from 1Hz to 200Hz
- Correction for sample capacitance and resistive losses

- **Air cooled quadrupole power supply for HCI**

The power requirement for HCI quadrupole is approximately 500W. Hence, it has been decided to design air cooled power supply instead of water cooled. The stability requirement of these power supplies is around 100 ppm. To achieve this stability, thermal management of the unit is critical, especially when it is air cooled design. High performance forced air cooled heatsink design of 1 kW capacity is in progress for unipolar and bipolar outputs.

- **Detector bias power supply (1 kV, 100μA)**

A 0-1 kV output range power supply with leakage current readback facility design has been finalized. This power supply can be used with solid state detector, charge particle detector and proportional counters. The implementation is in progress.

2.4.13 Servicing and maintenance support

BTS group provides time to time service and maintenance support for the following instrument.

- Target lab Vacuum unit deposition power supplies
  E-Beam source power supply (Model- TT3/6,Telemark)
  Atom Beam Source power supply (Model-850, Atomtech)
  e-Gun power supply (Model-922-0020, Varian)
- High voltage detector bias power supplies

Quad 1kV Bias supply (Model-710,EG&G Ortec)
5kV Detector Bias Supply (Model-659 EG&G Ortec)
3kV Detector Bias Supply (Model-556, EF&G Ortec)

- CAMAC Crate power supplies
  CAMAC Crate (Model-1502, Kinetic)
  CAMAC Crate (Model-6700-SCB, Bira Systems)

2.5 LOW ENERGY ION BEAM FACILITY (LEIBF)

G.Rodrigues, P.Kumar, P.S.Lakshmy, U.K.Rao, Y.Mathur, D.Naik, A.Mandal and D.Kanjilal

A. Source Operations

In the last academic year, an experiment was performed involving Bremstrahlung measurements with our ECR source. This was accomplished with the collaboration of scientists from IGCAR, Kalpakkam. We used a 1 inch NaI detector instead of a Ge detector due to its better efficiency to measure the x-rays over a wide energy range (upto a few MeV) from the injection side of the source. In fact, we measured these electron energies up to a few MeV. The measurements were carried out in two modes viz; beam tuning mode and without beam tuning mode. The measurements were carried out as a function of RF power, gas flow, bias voltage and extraction voltage. Figure 1(a) shows the set-up of the measurement and figure 1 (b) shows the x-ray spectra at different power levels. A complete analysis is underway.

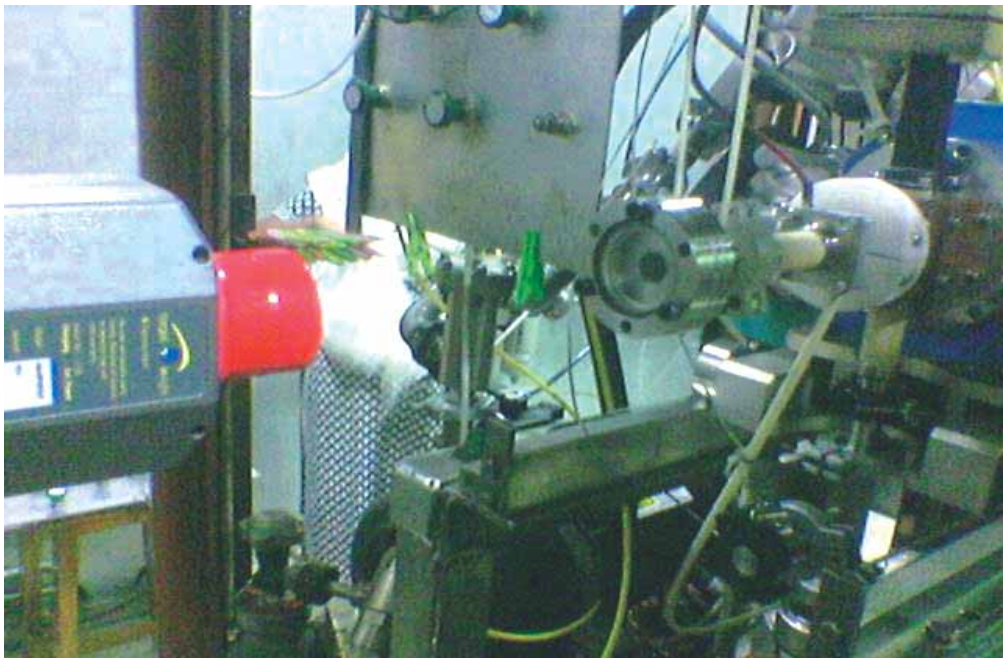

Fig. 1(a). Set-up of X-ray measurement at injection side of the ECR ion source

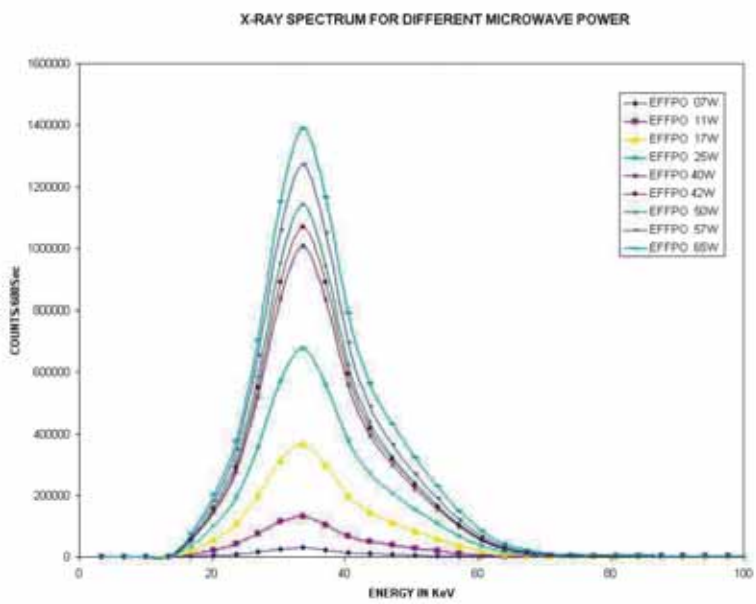

Fig. 1(b). X-ray spectra measured at different RF power levels

Fig. 2. View of the Einzel lens after it was found shorted

During normal operations, we found a short in the Einzel lens (see figure 2.) which was apparently due to sputtering of SS 304 material (see material lying next to the Einzel lens) from the last grounded cylinder (top portion, beam exit). This has been correlated with the huge currents beam extracted (and lost) and occasionally found that the body of the Einzel lens was getting hot. In future, a collimator will be installed in front of the lens and possibility of air-cooling will be

explored. New type of metallic beams are being developed using the oven, MIVOC, insertion and sputtering techniques. These beams are always found challenging to develop. They are mainly used for various kinds of materials science experiments and for gaining experience in ECRIS operation. Our goal is to develop these beams for future use in high current injector of superconducting linear accelerator (LINAC).

The complete beam optics has been worked out for the new LEIBF system. The complete design has been worked out and fabrication of new high voltage, double deck platform is ready for installation. Two additional beam-lines are planned and this requires a new switching magnet for this purpose. The design of the switching magnet has been finalized and order placed to DANFYSIK

The Low Energy Ion Beam Facility has been running almost full time for various experiments during the last year. A large no. of experiments related to atomic and molecular physics and materials science has been carried out. Typical experiments which have been carried out using the facility are listed below.

1. Formation of buried insulating layers in Si using high dose implantation of O and N.

2. Study of electrical, magnetic and structural changes induced by Ar implantation in polymers & nano-composites.

3. Study of multiple ionization of molecules by electron-ion-ion coincidences in ion TOF spectrometer using CH_4,CO_2,CO,SF_6 & CCl_4 targets.

4. Irradiation of Ar on silicon & in-situ measurements of I-V, C-V Schottky diode behaviour with varying dose.

5. Bremstrahlung measurements from ECR plasma as a function of gas pressure, rf power, bias voltage and extraction voltage with a)beam tuning b)without beam tuning.

6. Study of surface, luminescence, structural and optical properties on pure and doped LiNbO3 samples.

7. Experiments on molecular dissociation using CO and CH_4 targets.

B. Electronics Development

Two high voltage power supply modules of 3kV, 5mA were fabricated for electrostatic steerer in LEIBF. In the process of developing high voltage power supplies,we indigenously developed the high frequency transformer (figure 4.) for use in 10kV as well as 3kV power supplies. The high frequency transformer design parameters are as follows:

1. Output voltage (Vo) = 1.76kV
2. Turns of primary winding, Np = 10 turns
3. Turns of reset winding, Nr = 14
4. Turns of secondary winding, Ns = 1625 turns
5. Switching frequency (fs) = 50kHz
6. Maximum flux density (Bmax) = 220mT

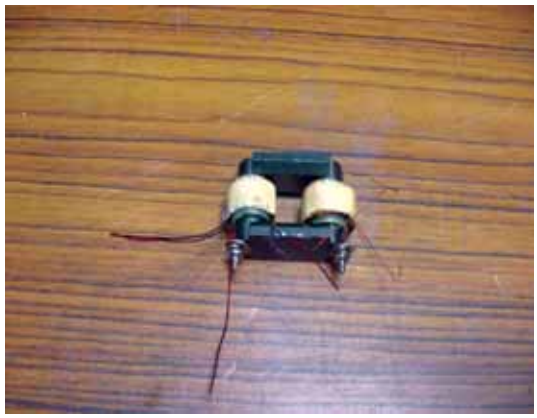

Fig. 4. View of the high frequency transformer

2.6 HIGH TEMPERATURE SUPERCONDUCTING ECRIS, PKDELIS AND LOW ENERGY BEAM TRANSPORT SYSTEM

G.Rodrigues, P.Kumar, P.S.Lakshmy, R.N.Dutt, U.K.Rao, Y.Mathur, D.Naik, A.Mandal, D.Kanjilal and A.Roy

A. Control system of PKDELIS ECR Source

Computerized control of all the systems of the High Temperature Superconducting Electron Cyclotron Resonance Ion Source (HTS-ECRIS) PKDELIS and low energy beam transport has been achieved. The control system is based mainly upon industry standard MODBUS RTU on RS485 and incorporates, among other features, a radio modem for easy high voltage deck control, a PLC for a flexible, connected and reliable interlock system, and client server based remote control. For low cost and ruggedness, industrial grade rail mounted modules are used. Due to the use of a PLC, the interlock signals are visible on the control program running on the PC and are available on the network as well. The actual system incorporates a local modbus connected to

Fig. 1. PKDELIS ECR ion source and Low Energy Beam Transport system (LEBT)

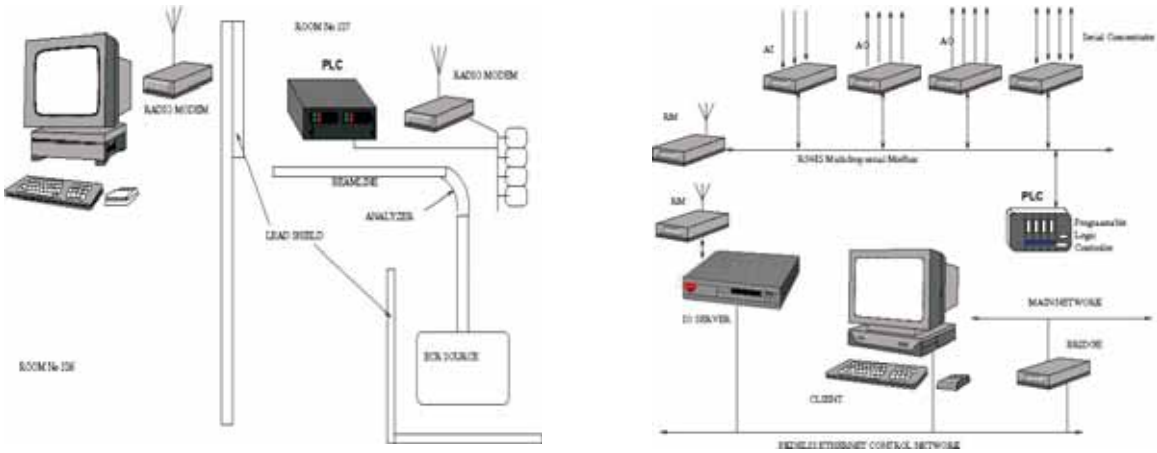

Fig. 2(a) Schematic of the control system **(b) Conceptual idea**

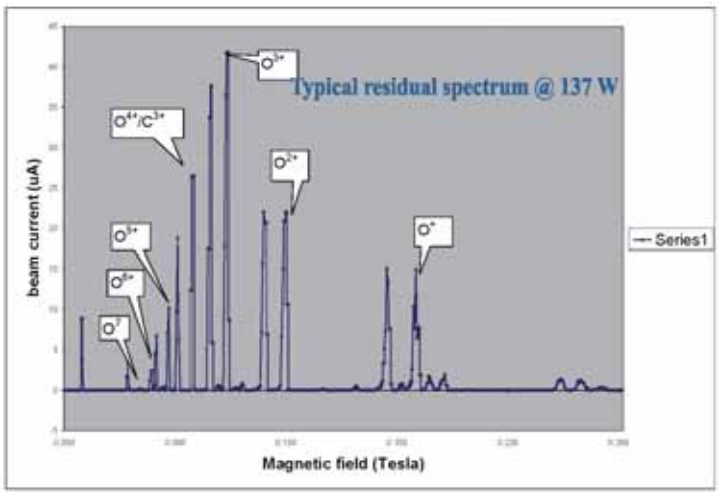

Fig. 2 (c) Typical residual spectrum taken from PKDELIS source

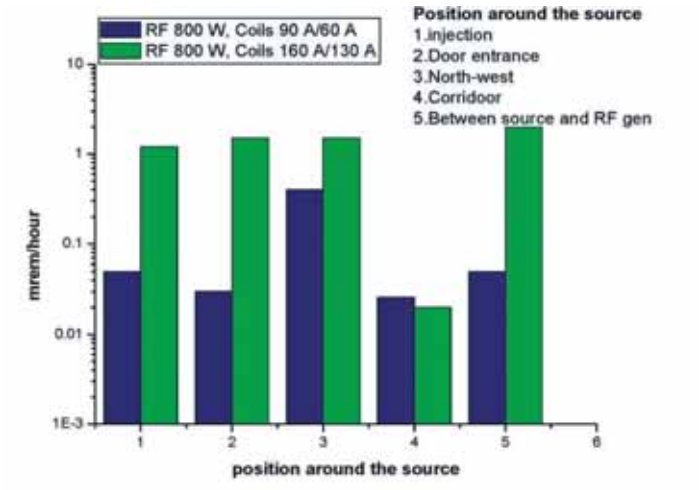

Fig. 3. Radiation shielding levels around the source

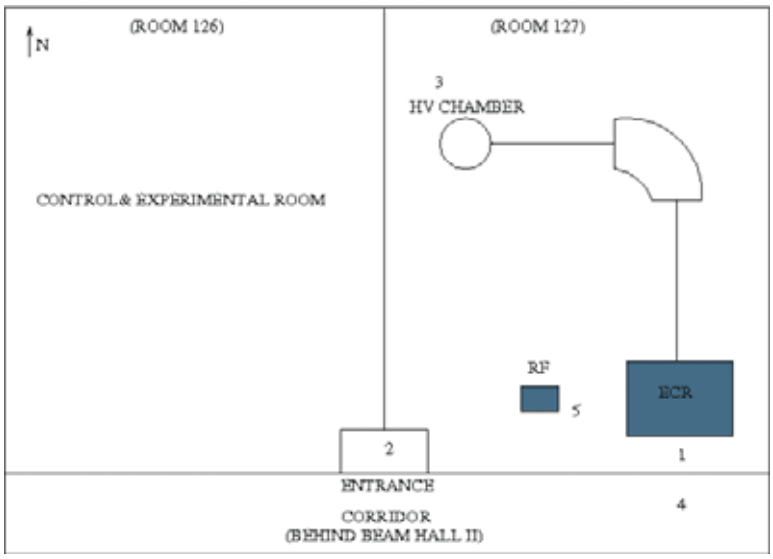

Fig. 4. View of layout of PKDELIS Source, LEBT and control area

the control server PC via a radio modem link. This is shown in figure 2. The control server PC also reads the PLC over the RS485 link. The control system will incorporate multiple RS485 buses and only the high voltage deck bus will be the one with the radio modem link. However, this is planned in the future and presently all the systems have a radio link. A simplified block diagram of the system is shown in the figure 2(a). The entire control is wireless to make the communication network noise free and to avoid the necessity of fibre optic cables especially for high voltage applications. The system has been running continuously and is found to be rugged under high voltage environments. A typical residual gas spectrum is shown in Fig. 2 (c).

B. Radiation Shielding

The radiation shielding of the HTS ECR source area has been completed especially plugging the leaks in the corners of the shielding manifold close to the source. This is shown in figure 3. Figure 4 gives an idea of the location of the shields located between positions 1 and 5. Shielding has also been done towards the north-west side (position 3) so that control and data acquisition can be carried out safely in room no.126 avoiding the high radiation levels in room no. 127.

C. Cryo-Cooler operations

The cryo-cooler on the extraction side was posing a severe cooling problem for the coil. We tried to remove the contaminant gas and re-charged it with 1 ppm of helium. This re-charging was carried out twice but the problem persisted. During the course of time, we also noticed that the sound of the cryo-cooler diminished when compared to the injection side which was running in a normal fashion. Therefore, we decided to open up the extraction cryo-cooler to investigate the problem. It was observed that the piston movement was restricted due to displacement of the flange which was not sitting symmetrically with respect to the piston. This impeded the motion and eventually could not cool down. A new part was replaced and the system was back into operation. A view of the damaged piston is shown in figure 5.

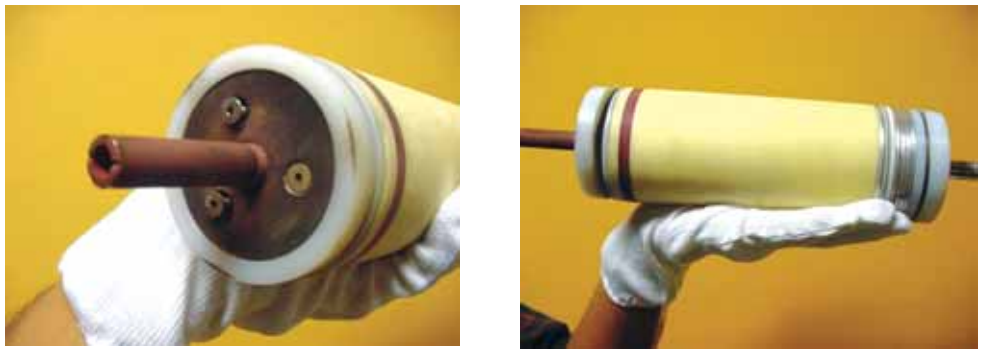

Fig. 5(a). End view of the piston with loose screws. (b) Side view

D. Development of new extraction system

A new, movable type, high current extraction system is presently under fabrication. This will facilitate in tuning the optics of various A/q beams under the influence of the strong axial magnetic field. The electrodes will be water cooled using de-ionized water. The pumping system will be mounted on the extraction tank to facilitate better vacuum close to the beam formation region. A series of ports will be mounted on the extraction tank body, one of them will be used for mounting a variable energy electron gun to study the effect of space charge neutralisation and alternately, another could be used to inject electro-negative gases into the system. This concept needs a careful study in order to limit the beam emittance. From simulations, it has been verified that the emittance can be reduced from 150 π mm.mrad to 100 π mm.mrad depending on the space charge neutralization fraction and the electron energy.

A 'large pole gap' magnetic steerer has been designed for correction of the beam mainly in the vertical direction. It would be placed after the extraction system to guide the beam through the analysing magnet. Due to the large acceptance of the beam line, the steerer has been designed with a large pole gap to give a deflection of more than 20 mrad. Additional cooling system is not required due to the low power dissipation at low designed fields. 3D code RADIA is being used to simulate the designed fields especially for large aperture, short length magnets.

E. Bremstraahlung measurements from PKDELIS ECR plasma

X-ray measurements have been carried out to understand the source performance. Typical axial bremstraahlung spectra measured at a distance of approximately one metre from the ECR plasma in the zero degree view port of the analysing magnet at a fixed rf power of 300 W is shown in figure 3. A small Si pin diode detector (AMPTEK) was used with proper collimation to obtain the x-rays only from the plasma. From these measurements, we found that as the mirror ratio is increased on the injection and extraction sides, the slope of the distribution changed considerably. The legend in figure 6 shows the values of the injection and extraction coil currents used to change the mirror ratio at fixed rf forward power level of 300 W. This shows that a single electron temperature component is found to increase with higher mirror ratios. All measurements were performed for a fixed time period of 900 seconds. The energies of the x-rays which span from a few tens of keV to a few hundred keV show that at these power levels the energies of the x-rays correspond to the available electron energies. We expect that at higher power levels higher energy

electrons would be produced, but these measurements could not be completed due to problems with the DC waveguide break at higher levels of RF power. We have also measured the bremstraahlung in the radial direction. These measurements however show a 'two-component' electron temperature. This requires more detailed measurements for in-depth understanding of the behaviour of the plasma.

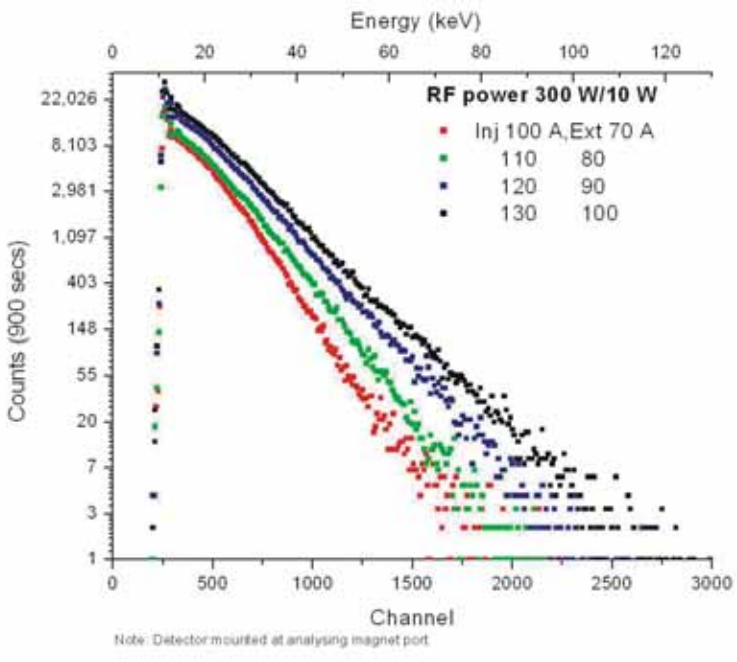

Fig. 6. Axial bremstraahlung measurements from PKDELIS ECR plasma

F. Low Energy Beam Transport

The LEBT of the High Current Injector consists of the High Temperature Superconducting ECR source PKDELIS, multi-electrode extraction system/solenoid/magnetic quadrupole doublet, 90° analysing Magnet, 400 kV high voltage accelerating column and a few focussing devices to transfer the beam from ECR to RFQ entrance. A large acceptance analysing magnet has been designed to analyse ions from the ECR source. This magnet will be placed on the high voltage platform to reduce beam loading of the high voltage power supply. The combined function magnet has been designed to incorporate higher order terms to reduce the higher order aberrations. Since the technical challenge of transporting low energy, high current ions lies mainly in the low energy section of the injector, utmost care has been taken in the design of the LEBT. The ions from the ECR source are first extracted around 30 kV and A/q analysed by a large acceptance analysing magnet and further accelerated using deck voltage with a maximum allowable voltage of 400 kV. The energy of this beam will be further accelerated by a Radio Frequency Quadrupole accelerator (RFQ), Drift Tube LINAC (DTL) and low β cavity resonators to match the existing LINAC beam-input energy requirements. A new beam hall is being constructed on the east side of the present beam hall I to house these facilities. The ion optical design has been carried out considering the beam input parameters of maximum A/q = 10 and beam emittance of 200 π mm.mrad. A

second order corrected beam optics on the 400 kV high voltage platform and upto the RFQ entrance is shown in figure 7 for E/q= 380 kV.

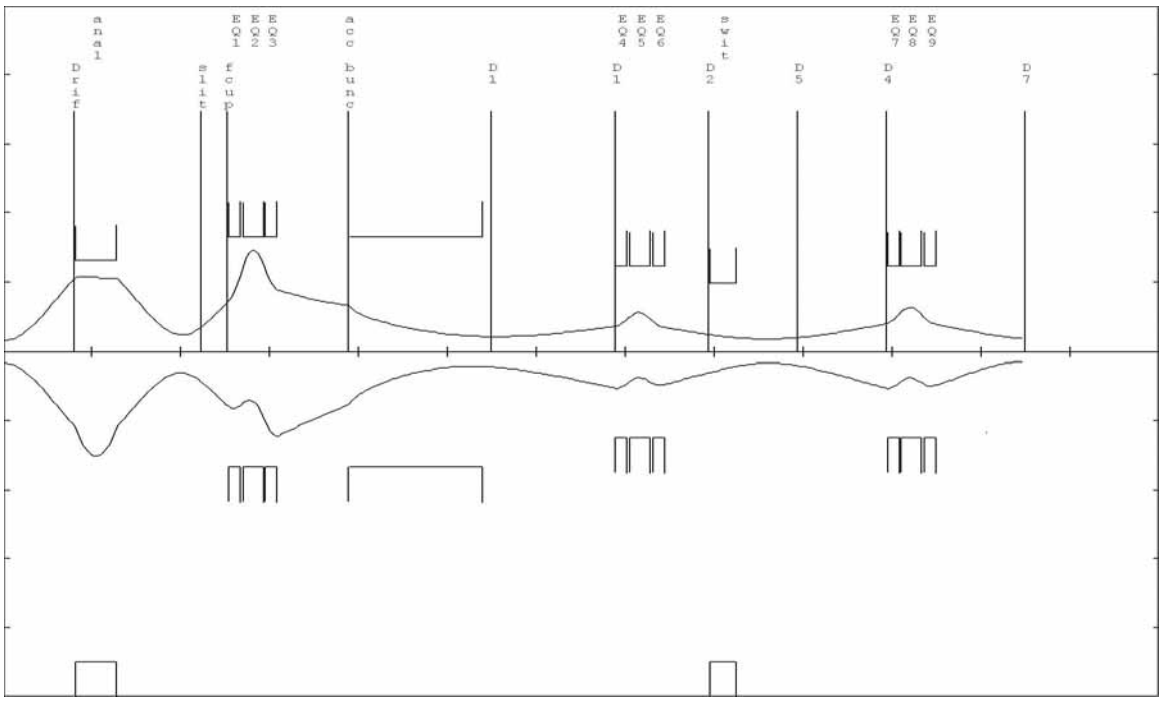

Fig. 7. Second order corrected beam envelope from ECR source upto RFQ entrance for E/q = 380 kV

2.7 PRELIMINARY RF TEST ON THE INITIAL UNMODULATED PROTOTYPE RFQ ACCELERATOR

C.P. Safvan, Sugam Kumar, R. Ahuja, A. Kothari, D. Kanjilal and A. Roy

The proposed 48.5 MHz Radio Frequency Quadrupole (RFQ) is designed to accelerate ions with A/q of 7 from 8 keV/A to 180 keV/A. The RFQ structure is 4 m long and vane posts support the vane shaped rods. An initial unmodulated 1.17 m prototype of the 48.5 MHz RFQ is designed, constructed, installed and studied to determine the final specifications for modulated RFQ accelerator. The ion beams produced by the ECR (PKDELIS) source will be injected into the RFQ and be further accelerated to just below 1MeV/A by a drift tube LINAC (DTL) working at room temperatures, before being further velocity matched with a low beta cavity into superconducting LINAC, which will further accelerate the ions.

The final cavity structure has been manufactured at Don Bosco Technical Institute's Workshop. A view of the prototype RFQ is shown in Fig.1. The cavity is equipped with various ports where the input inductive loop for power coupling and output loop for probe is installed. The system is able to achieve high vacuum level (10^{-7} torr) with the help of a single turbomolecular pump. The RFQ vanes and vane supports were being fabricated at Indo-German Tool Room

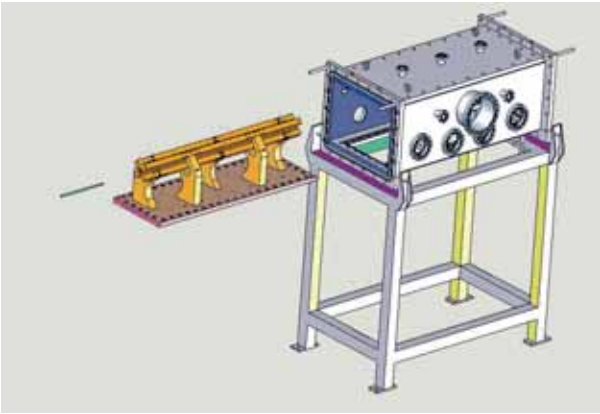

Fig.1. General assembly of the RFQ at IUAC

Indore and Ahmedabad. The whole electrode assembly is inserted in RFQ cavity.

Following the mechanical alignment the vanes were installed and the measurement of parameters like resonant frequency (f0), Quality factor (Q0), Shunt impedance (R), Power required, Quadrupole symmetry and Electric field mapping is being done. A fully automated bead puller system is developed. The bead pull and capacitive variation method is being used with the help of Self Exciting Loop (SEL) and Network Analyzer for the purpose RF parameters measurement. SEL is used to minimise the possible long-term temperature drift while measuring the frequency shift. The bead consists of 2 mm diameter on fishing thread of 0.28 mm diameter. The bead is dielectric spherical in shape, which is exclusively sensitive to the electric field. The frequency shift along the length of cavity is shown in Fig.2.

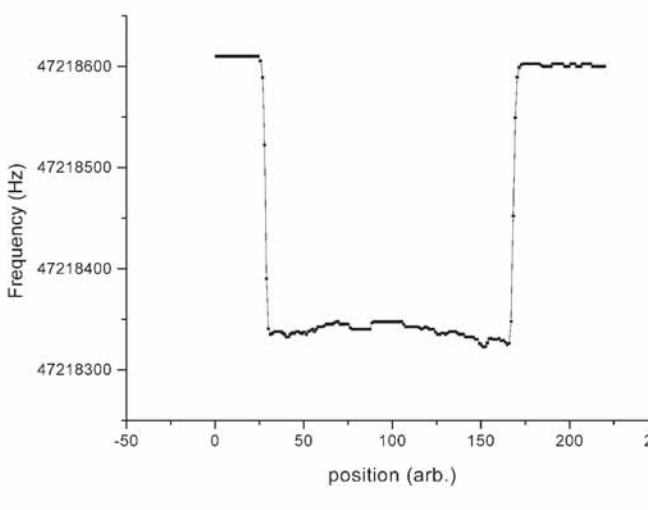

Fig.2. The shift in the resonance frequency plotted vs. cavity length for fundamental mode.

The resonance frequency and quality factor measured was 47.2234MHz and 1046 respectively, while shunt impedance is found to be 21.8 k-ohm. Two independent measurements have been done in the azimuthal plane to check the quadrupole symmetry and the electric field distribution in this plane. Fig.3.shows the results of bead pull along the azimuthal plane.

The quadrupole electric field strength in quadrant 1 is found to be roughly 3.8% higher while of quadrant 2 is 10.4% lower than the average electric-field strength of the quadrant 3 and 4. These results indicate that the distribution of the electric field is symmetrical within the beam radius and tend to asymmetrical in region greater than the beam radius.

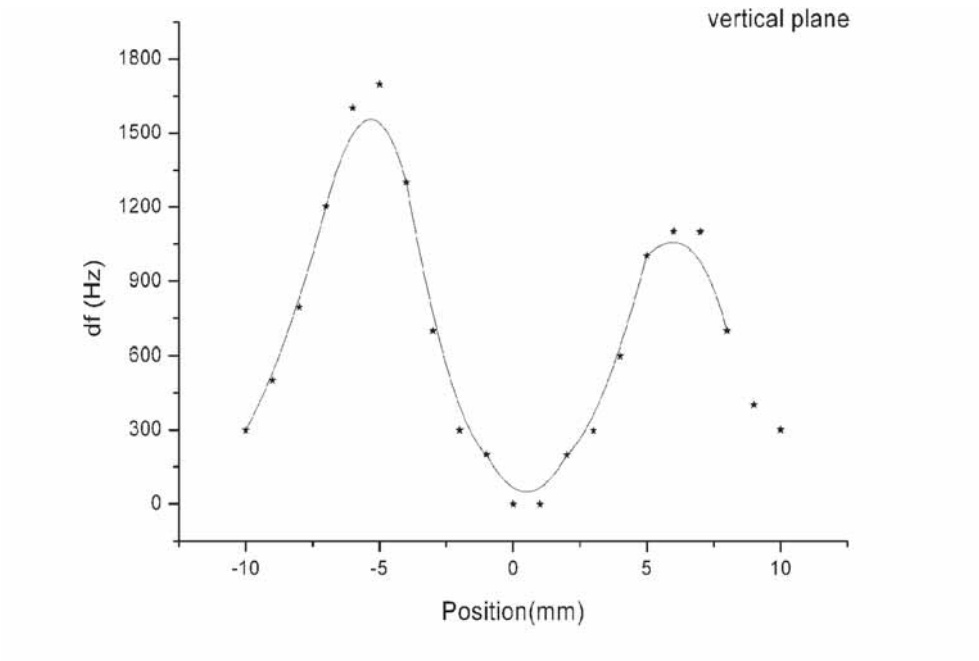

Fig.3.Quadrupole symmetry in azimuthal plane